EFFECTIVE PERMEABILITY OF CARBONATE RESERVOIRS USING THE RANDOM FINITE ELEMENT METHOD

D.V. Griffiths
d.v.griffiths@mines.edu
Colorado School of Mines, Golden, CO, USA
University of Newcastle, NSW, Australia
Jumpol Paiboon
jpaiboon@mines.edu
Colorado School of Mines, Golden, CO, USA
Jinsong Huang
Jinsong.Huang@newcastle.edu.au
University of Newcastle, NSW, Australia
Gordon A. Fenton
Gordon.Fenton@Dal.Ca
Dalhousie University, Halifax, NS, Canada

Abstract. *The purpose of the study is to investigate the influence of porosity and void size on the effective permeability of carbonate reservoirs. A random finite element method (RFEM) has been developed involving an ideal block of material leading to direct evaluation of the effective permeability. The approach involves a combination of finite element analysis and random field theory. Following Monte-Carlo simulations, the mean and standard deviation of the effective permeability can be estimated leading to probabilistic conclusions about flow characteristics. The influence of block size and representative volume elements (RVE) are also discussed and a comparison is made between the effective permeability of isotropic and anisotropic reservoirs.*

Keywords: Random finite element method (RFEM), Representative volume element (RVE), Effective permeability, Homogenization

1. INTRODUCTION

Over millions of years, various kinds of microscopic creatures have died, piled up at the bottom of the sea and become part of the sediment that eventually turns into shale. The heat from deep inside the earth then turns their bodies into hydrocarbons, i.e. oil and natural gas. With the intense pressure of the earth, the oil and gas are squeezed out of the shale and gather together and

may literally drift. Finally, they may become trapped in rock such as sandstone or limestone. Limestone is a kind of sedimentary rock, derived from the composition of plants and animals that secrete calcium to form their skeletons; thus limestone is a type of rock made up mainly of calcium carbonate. Limestone is a rock that has a large economic value; for example, it is used as gravel for construction. More importantly, it is a reservoir of petroleum. One-third to half of the amount of oil comes from these limestone and dolomite. Despite the hard and solid macroscopic appearance of sandstone or limestone, it is in fact porous, hence, trapping fluids such as oil or natural gas.

Porosity and permeability are properties of any rock or loose sediment. Porosity is a normalized measure of the volume of void spaces where the oil or gas may be held; thus the rock's ability to hold a fluid. Permeability is a characteristic that determines the ease with which oil and gas can flow through the rock. The permeability of a rock refers to the rock's resistance to fluid flow. A rock is said to have "low permeability" when it is harder for fluid to pass through it. If fluid passes through the rock easily, it is said that the rock has "high permeability". The movement of petroleum is similar to the movement of groundwater. In the form of crude oil and/or natural gas, petroleum moves through the spaces within the rock and gathers in region with higher porosity. Since natural gas and oil are lighter than water, they separate themselves from water, then rise and accumulate above the water. The movement of the gas and oil stops when the gas and oil reach a non-permeable layer. Thus, porosity and permeability are absolutely necessary for good-quality production of oil or gas.

Even if the expected porosity of the site can be conservatively estimated, void locations may be unknown. In addition, two sites with the same porosity may have quite different void sizes, where one has numerous small voids and the other fewer large voids. To facilitate the modeling of boundary value problems, the goal of this work is to determine the effective properties of such materials. In this paper the property of interest is the permeability and the effective properties are defined as those properties that would have led to the same response if the material had been homogeneous. The behavior of a heterogeneous material with a micro-structure, consisting of varying properties, has been studied by a number of investigators using experimental, analytical and numerical methods. The macro-scale of a homogeneous material, which has a heterogeneous micro-structure on the micro-scale level, is investigated in order to address the issue of how the microstructure affects the material on the macro-scale. The goal of homogenization is to obtain the overall (effective or equivalent) properties to represent the macro-scale properties. An important objective of micro-mechanics is to link mechanical relations going from finer to coarser length scales. A useful concept in this homogenization process is the representative volume element or RVE. An RVE is an element of the heterogeneous material that is large enough to capture the effective properties in a reproducible way. From an efficient modeling point of view, the smallest RVE that can achieve this is of particular interest (e.g. Liu 2005).

Homogenization approaches based on theoretical and numerical methods have been developed for assessing RVE size. Several reviews have been proposed for describing different homogenization approaches (e.g., Klusemann and Svendsen, 2009; Mercier et al., 2012). Bourgeat (1984) considered the behavior of two-phase flow in a periodically fractured porous medium. Saez el at. (1989) proposed macroscopic equations to the processes of one and two phase flow though heterogeneous porous media. The Self-Consistent approach (Pozdniakov and Tsang, 2004) involved estimating the effective hydraulic conductivity of a heterogeneous medium and was applied to a fractured porous material. Moreover, there have been several theoretical approaches developed to assess effective permeability (e.g., Hashin and Shtrikman, 1963; Ostoja-Starzewski et al., 2007; Pouya and Vu, 2012).

Numerical methods of homogenization have been used to validate some of the theoretical approaches. Holden and Lia (1992), for example, proposed an estimator for an effective permeability tensor based on a one-phase incompressible flow. The estimator worked for all kinds of heterogeneous reservoirs. Waki et al. (2005) considered the magnetic interaction between inclusions to estimate the effective permeability of magnetic composite materials. Held el at. (2005) presented numerical results of the effective flow and transport parameters in heterogeneous formations. Szymkiewicz (2005) presented an approach to calculate the effective conductivity of a heterogeneous soil for periodic media with inclusions of various shapes. Muc and Barski (2008) presented an introduction on the prediction of the effective permeability. Popov et al. (2008) applied the Stokes-Brinkman equation as a fine-scale model for flow in vuggy, fractured karst reservoirs. Barski and Muc (2011) considered the possibility of theoretical predictions of effective properties in 2D and 3D. Some of these numerical methods of homogenization were compared with the theoretical results.

Several different approaches have been used in the past for studying the porosity-permeability relationships in various reservoir rocks. The porosity and pore size distribution are both important factors in determining fluid flow characteristics through porous media (Kate and Gokhale, 2006) and there are various approaches for estimating pore size distribution. For example, Jiru et al. (2010) considered the pore size distribution of rocks and soils with a scanning electron microscope and Abedini et al. (2011) proposed a statistical approach to the pore size distribution with reservoir rock. The Lattice Boltzmann method (LBM) is a versatile method for simulating flow in porous media. Direct LB simulation on micro scale 3D image data offers a potential for understanding fluid flow processes in a material with complex microstructure (e.g. White et al. 2006). Ramtad et al. (2011) recently proposed a study of relative permeability functions derived from two-phase Lattice Boltzmann simulations on X-ray microtomography pore space images of sandstone. Many theoretical and numerical studies of the LBM are becoming an accepted approach in the fluid flow of porous material. (e.g., Bosl et al., 1998; Guo and Zhao, 2002; Zhang, 2011 and Grucelski and Pozorsky, 2012). Nuclear Magnetic Resonance (NMR) imaging is an advanced approach to imaging pore space in a saturated rock with a nuclear magnetic moment. A limitation of the NMR is that if the porosity is not very large, the amount of water present in a saturated porous rock is small, which results in weak signal intensity. (Edie et al., 2000-11). Hidajat et al. (2001) considered the permeability of spatially correlated porous media computed by the LBM and the formation factors of generated porous media is solved by Laplace's equation. There are studies relating to the characterization of fluid flow in porous media by NMR approaches. (e.g., Liaw et al., 1996; Kimmich, 2001; Sørland et al. 2007; Jin et al. 2009). The X-ray computed tomography (Micro-CT) creates a representation of rock microstructure. The approach involves three main processes; 3D imaging at the required resolution, segmention of the 3D imaging and computer simulations of fluid flow for permeability (Sharp et al., 2009). The Micro-CT has become an important technique for characterizing porous materials. (See also Zhang et al. 2009; Kalem, 2012).

Although there have been many theoretical and numerical approaches, the results are rather unsatisfactory because of the uncertainties in the characterization of the geometry changing from place to place, horizontally and vertically. The RFEM is an alternative approach for modeling the influence of inclusions and voids in geomaterials. The method can be used to estimate the effective properties of materials with randomly distributed voids. The RFEM, first developed by Griffiths and Fenton (1993) and Fenton and Griffiths (1993), has been applied in numerous studies of geotechnical engineering (e.g. Griffiths and Fenton 2007, Fenton and Griffiths 2008). In this research, conventional finite element analysis (e.g. Smith et al. 2014) was combined with

random field generation (e.g. Fenton and Vanmarcke 1990, Fenton and Griffiths 2008) and Monte-Carlo simulations to develop output statistics of quantities such as effective permeability. Through control of the spatial correlation length, both the volume and size of voids could be considered by the RFEM. Paiboon et al. (2013) recently proposed the RFEM in the homogenization of geomaterials containing random voids. The first part of the work investigates the statistics of the effective permeability in 3D as a function of porosity and void size, and compares the results with other investigators. Effective permeability with an anisotropic void structure is also considered. The second part of the work investigates the size of the RVE for different input void properties. Of particular interest here is the number of Monte-Carlo simulations needed for stable results as a function of the size of the RVE under consideration.

2. FINITE ELEMENT MODEL

The random finite element method (RFEM) combines finite element methods and random field theory. In this work, finite element analysis of a 3D cube of elastic material using 8 node hexahedron elements is combined with random field generation and Monte-Carlo simulations to model a porous material containing voids. The goal is to develop output statistics of the effective permeability for different void sizes and porosity. Examples of the model are shown in Figure 1.

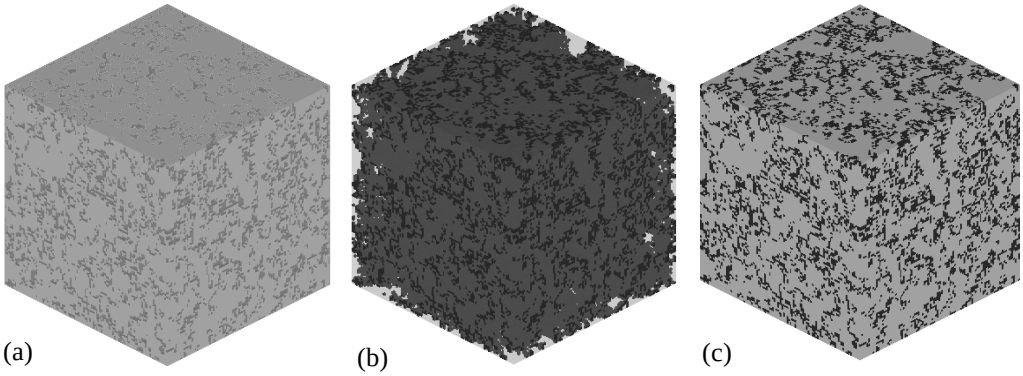

Figure 1 The 3D finite element model of ideal cubic blocks with mesh $100\times100\times100$: (a) the material, (b) the voids, and (c) the combined model which show dark and light regions indicating voids and material respectively

The finite element mesh for this study consists of a cubic block of material of side length $L=1$ modeled by $100\times100\times100$ 8-node cubic elements of side length $\Delta x=\Delta y=\Delta z=0.01$. Any consistent system of units could be combined with the dimensions and properties described in this work. Each node has one degree of freedom (the fluid potential at that position). A constant fixed potential of one and zero are fixed on the back right and front left faces respectively. All other faces are considered impermeable. No internal sources or sinks are considered. Figure 2 shows a cubic element test of the permeability block model with random voids. The finite element method can then solve the equation to obtain the fluid potentials across the ideal permeability block. Because a mesh such as this involves rather large global matrices, the equation solution in the runs described in this work will be performed using a preconditioned conjugate gradient (PCG) technique with element-by-element products as described by Smith et

al. (2014) which avoids entirely the need to assemble the global permeability matrix. Once the flow rates Q has been calculated, the effective permeability K, is given by

$$K = \left(\frac{Y_L}{X_L Z_L} \right) \left(\frac{Q}{H} \right) \tag{1}$$

where H is the head difference between the upstream and downstream faces (=1), and X_L, Y_L and Z_L are the side lengths of the permeability block (all =1).

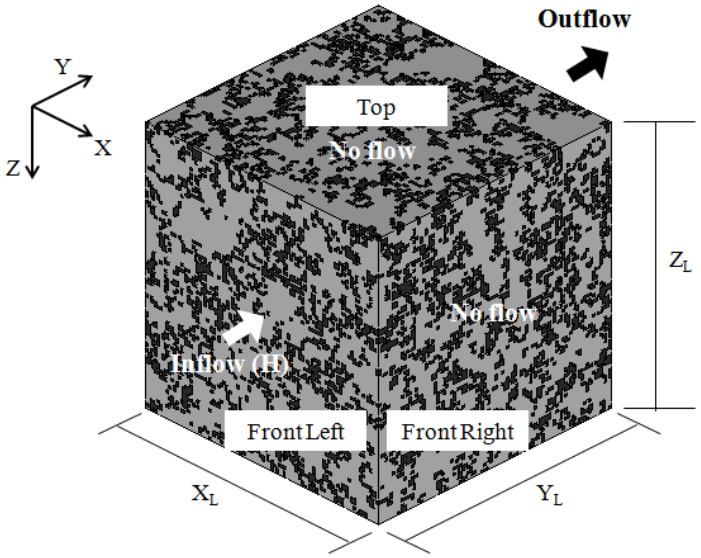

Figure 2 A "cubic element test" of the permeability block model with random voids portrayed by the dark and grey elements represent, respectively, voids and intact permeability material. A constant head difference ($H = 1$) is applied to the back right and front left boundary. The top, bottom, front right and back left boundaries are impermeable.

3 CONTROLLING THE VOID SIZE

The random field generator in the RFEM model known as the Local Average Subdivision method (LAS) (Fenton and Vanmarcke 1990) is used to model spatially varying void properties. The targeted mean of porosity n is based on the standard normal distribution shown in Figure 3, and the spatial correlation length θ is used to control the void size. A single value of the random variable Z is initially assigned to each element of the finite element mesh. Once the standard normal random field values have been assigned to the mesh, cumulative distribution tables (suitably digitized in the software) are then used to estimate the value of the standard normal variable $z_{n/2}$, for which

$$\Phi\left(z_{n/2}\right) - \Phi\left(z_{-n/2}\right) = n \tag{2}$$

where Φ is the cumulative normal distribution function, and n is the target porosity.

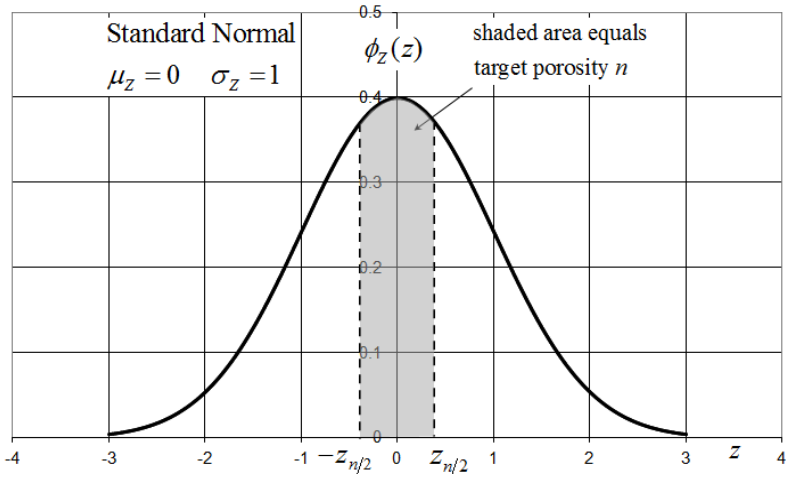

Figure 3 Target porosity area in 3D standard normal distribution of random field

Thereafter, any element assigned a random field value in the range $|Z| > z_{n/2}$ is treated as intact material with a permeability given by K_0, whereas any element where $|Z| \le z_{n/2}$ (shaded area in Figure 3) is treated as a void element with an assigned permeability of $K_0^{'} = 100$ (100 times larger than the surrounding intact material). The void size in this study is controlled by the random field spatial correlation length θ which incorporates a "Markov" spatial correlation structure as follows

$$\rho(\tau) = \exp\left(-2|\tau|/\theta\right) \tag{3}$$

where ρ = the correlation coefficient; $|\tau|$ = absolute distance between points in the field; and θ = scale of fluctuation or spatial correlation length. Larger values of θ will lead to larger voids and vice versa.

The Markov equation delivers a spatial correlation that reduces exponentially with distance. For example, according to Equation 3, $\tau < \theta$, the correlation coefficient $\rho > 0.13$. In the current study, ρ varies from 0 to 1. Points close together are strongly correlated and therefore likely to belong to the same void. In the limiting case of $\theta \to 0$, the random field value changes rapidly from point to point, delivering numerous small voids. At the other extreme as $\theta \to \infty$, the random field value on each simulation becomes increasingly uniform, with some simulations representing entirely intact material and other consisting entirely of voids. For example as shown in Figure 5, the models show typical simulations of different void clustering for two materials with the same mean porosity. In this study, the spatial correlation length is expressed in dimensionless form.

$$\Theta = \frac{\theta}{L} \tag{4}$$

where L is the side length of the permeability block ($L = 1$)

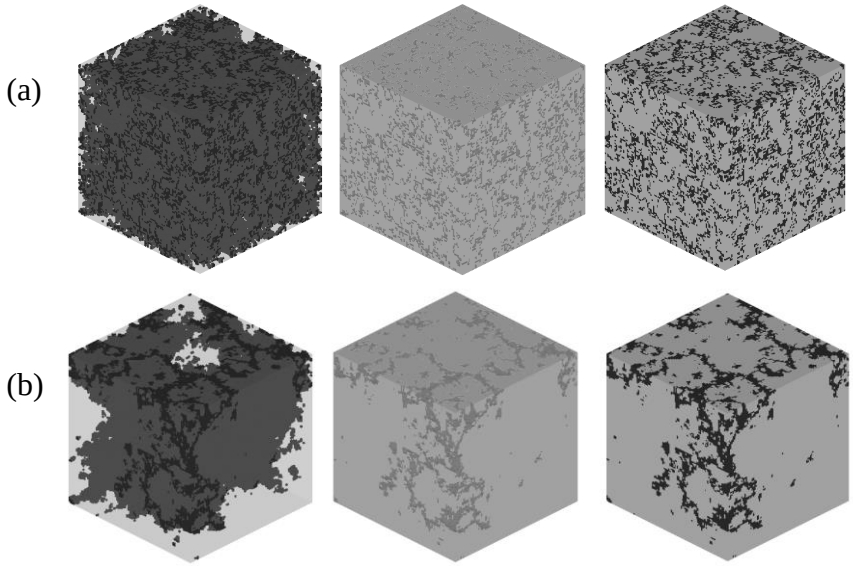

Figure 5 Typical simulations showing generation of voids at low (a) and high (b) spatial correlation lengths θ (mesh 100×100×100 and $n = 0.2$ in both cases)

4 MONTE-CARLO SIMULATIONS

A "Monte-Carlo" process is combined with the RFEM and repeated until stable output statistics are achieved. The primary outputs from each analysis is the total flow rate Q. Although each simulation uses the same Θ and n, the spatial location of the voids will be different in each simulation. Thus, in some cases, the voids may include few large volume voids, while the others could include many frequent smaller volume voids. Following each simulation, the computed flow rate Q is converted into "effective" values of permeability as shown in Equation 1. Each effective permeability value is then normalized as K / K_0 by dividing by the permeability of material K_0. In the current study, following some numerical experiments, as shown in Figure 6, it was decided that 1000 simulations for each parametric combination would deliver reasonably repeatable results.

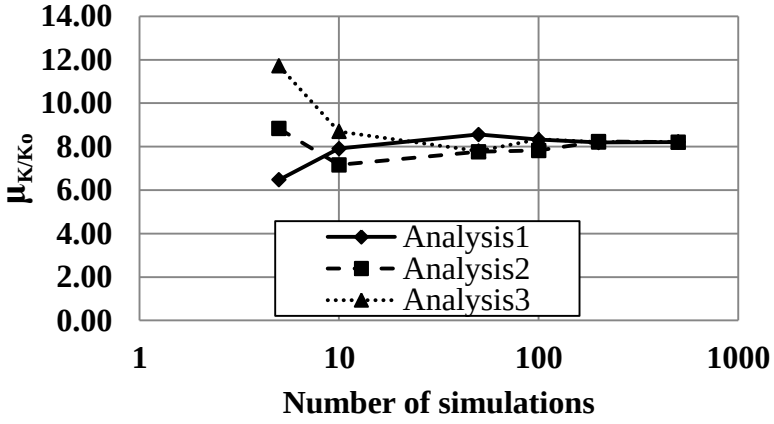

Figure 6 Sensitivity of the mean effective permeability as a function of the number of simulations for $n = 0.2$ and $\Theta = 1.0$

5 RESULTS OF RFEM

Following each set of 1000 Monte-Carlo simulations, the mean and standard deviation of the normalized effective permeability were computed for a range of parametric variations of n and Θ, with results shown in Figures 7 and 8, respectively.

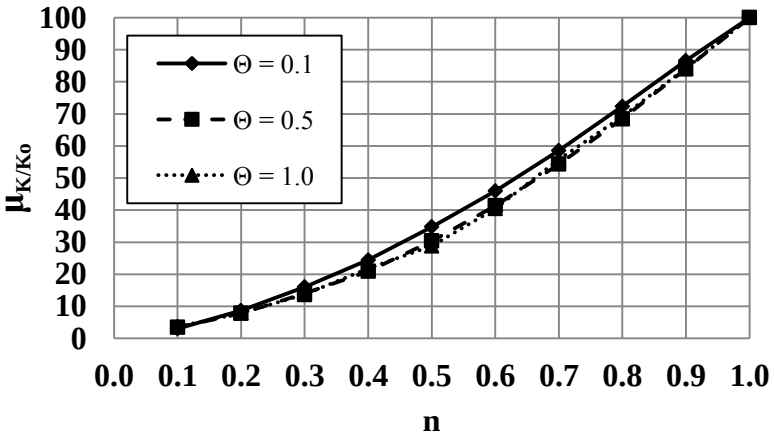

Figure 7 μ_{K/K_0} vs. n for Θ = 0.1, 0.5 and 1.0

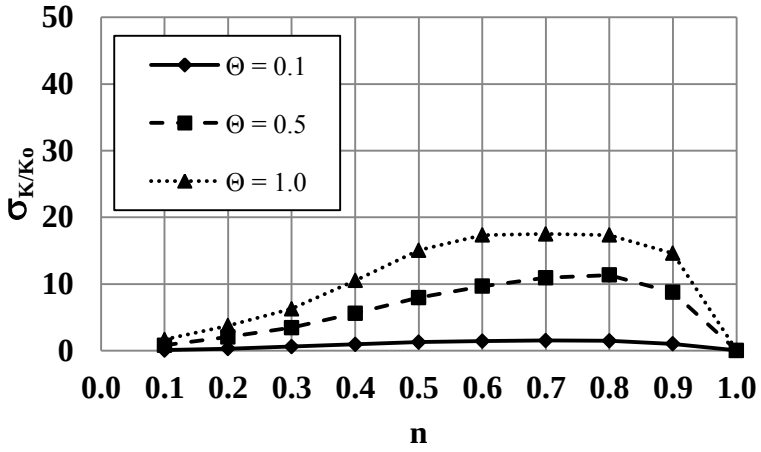

Figure 8 σ_{K/K_0} vs. n for Θ = 0.1, 0.5 and 1.0

It can be noted from Figure 7 that the mean normalized effective permeability increases towards one hundred with increasing porosity n and that Θ does not have much influence. Figure 8 shows that Θ has more influence on the standard deviation of the effective permeability σ_{K/K_0}. The standard deviation values as $n \to 0$ (intact permeability material) and $n \to 1$ (void material) show very low variance since almost all simulations are the same and model essentially uniform material. The standard deviation was observed to reach a maximum value at around $n \approx 0.7$.

6 REPRESENTATIVE VOLUME ELEMENT (RVE)

An RVE is an element of the heterogenous material is large enough to represent the microstructure but small enough to achieve efficient computational modeling. The RVE study considered four cases as shown in the results of Figure 10. Figure 9 shows a sequence of five blocks contained within and including the largest block of dimensions $1.0 \times 1.0 \times 1.0$. The different block sizes will indicate the optimal RVE for the given input conditions. When the RVE is "big enough", it was expected that the standard deviation of the effective permeability would be reduced and its mean essentially constant, as shown in Figures 10(a) and 10(b). The statistical results of each set of Monte-Carlo simulations are shown in Figure 9

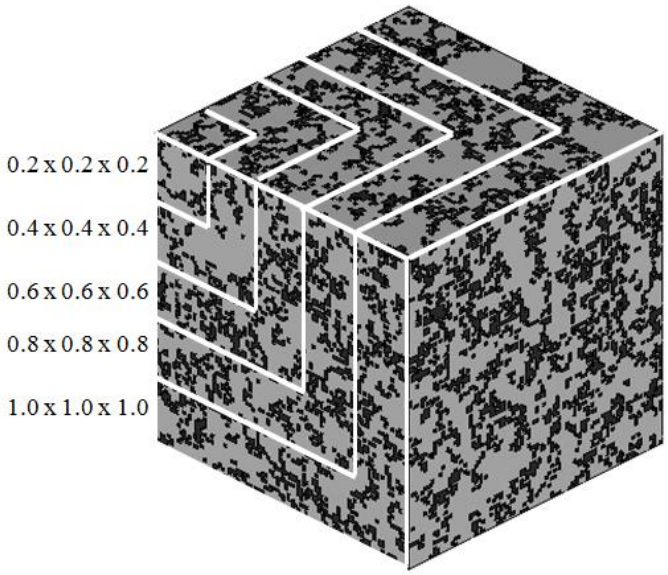

Figure 9 Different block sizes for computing the effective permeability of a material with random voids

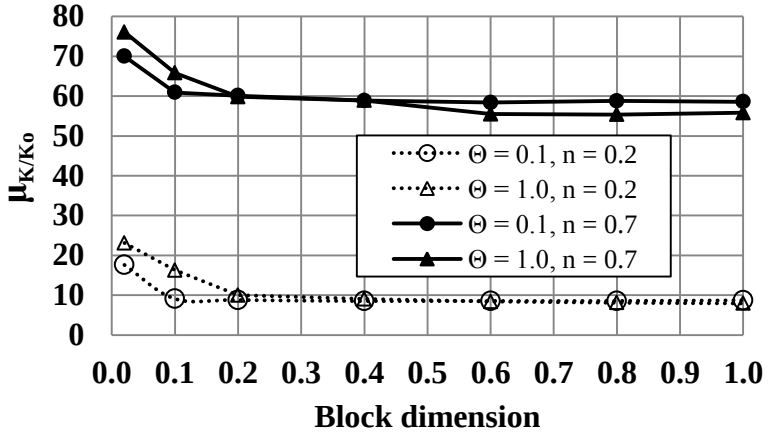

(a)

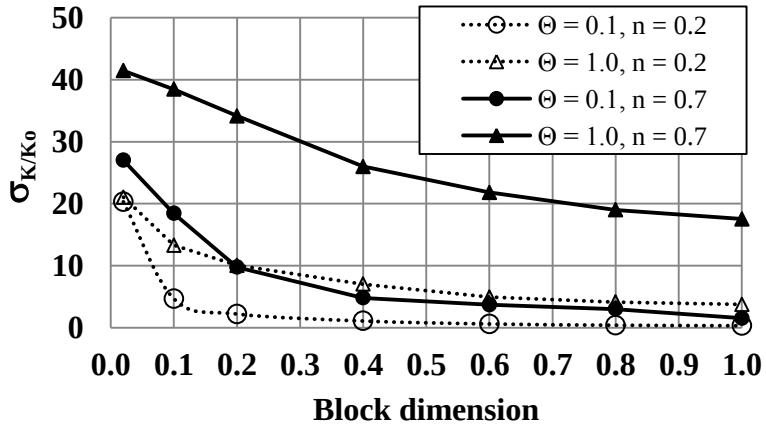

(b)

Figure 10 Effective permeability (a) mean and (b) standard deviation following 1000 simulations for different block sizes

The mean values plotted in Figure 10(a) are fairly constant for different block sizes, however the higher values of Θ seem to require a larger RVE before they become constant. The standard deviation shown in Figure 10(b) displays more variability with block size and tends to zero as the blocks get bigger, but at a slower rate for higher values of Θ. In both Figures 10, it is noted that the influence of Θ on block statistics is greater than that of n. The RVE depends more on spatial correlation length (void size) than porosity.

7 COMPUTER RESOURCES AND TIMINGS

A desktop with an Inter Core i7-2600 CPU @ 3.4 Ghz Ram: 8 GB was used to obtain all of the results presented in this research. Figure 11 shows the CPU time used for different block sizes. The results show that the CPU time depends on porosity and spatial correlation length. At a $100\times100\times100$ mesh, the CPU time for the low porosity and high spatial correlation length case was about 480 hours, while for a high porosity and low spatial correlation length it was more like 150 hours. The reason for this discrepancy is thought to be the slower convergence observed in the iterative solvers when there is more variability present in the permeability matrices with low void content.

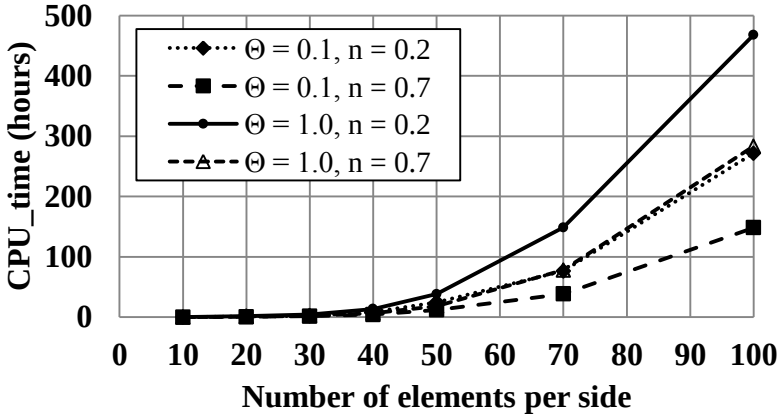

Figure 11 CPU timing for different block sizes with 1000 simulations

8 COMPARISON OF 3D ISOTROPIC AND ANISOTROPIC MODELS

In this section, 3D anisotropic models are considered for comparison with isotropic models. In the 3D isotropic case, the spatial correlation length of voids is set as $\Theta_x = \Theta_y = \Theta_z = 0.1$. Figure 12 shows how voids are elongated in the anisotropic direction. From Figure 13, it is seen that the effective permeability is greatest when voids are elongated in the direction of flow. Thus the effective permeability is greatest when $\Theta_y >> \Theta_x = \Theta_z$

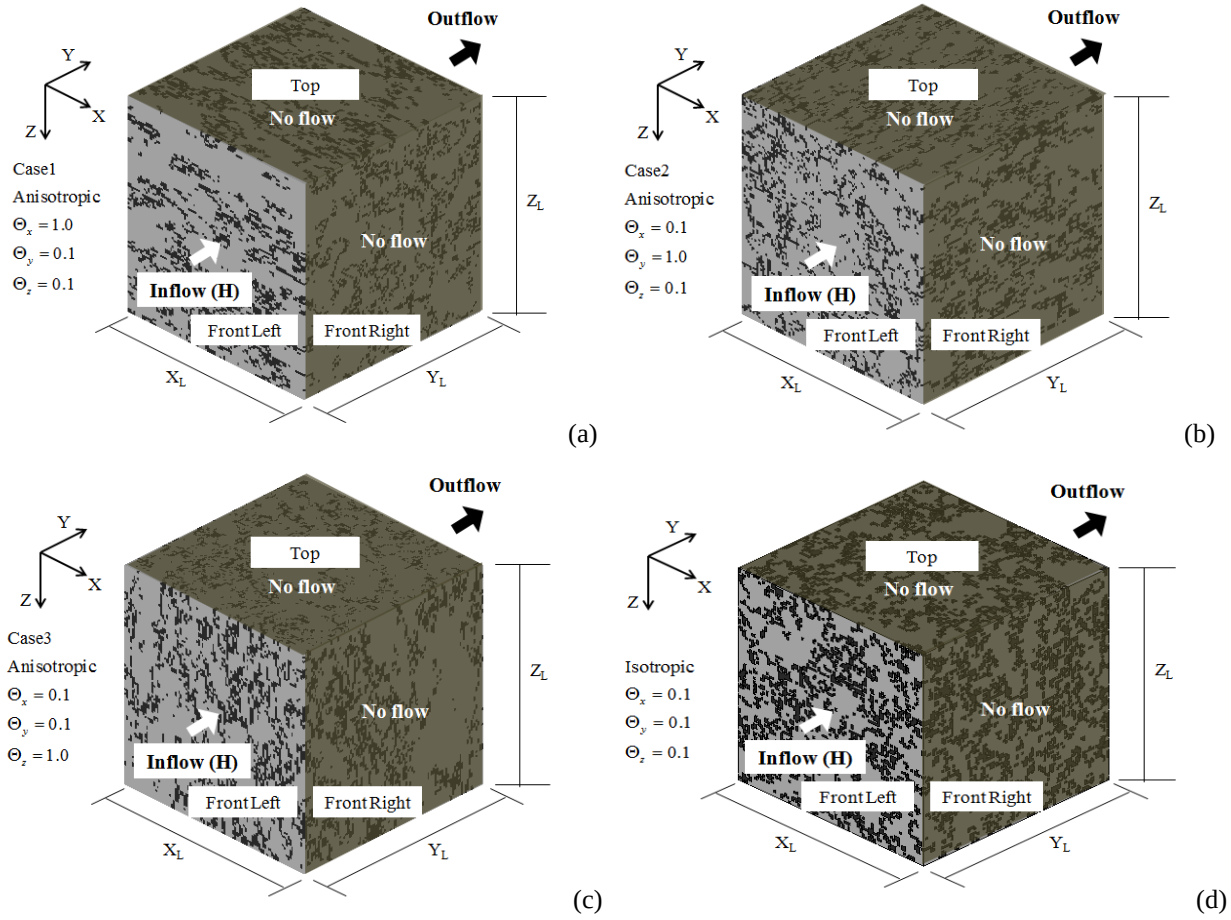

Figure 12 Typical simulations showing the generation of voids: (a) anisotropic model with $\Theta_x = 1$, (c) anisotropic model with $\Theta_y = 1$ (c) anisotropic model with $\Theta_z = 1$ and (d) isotropic model

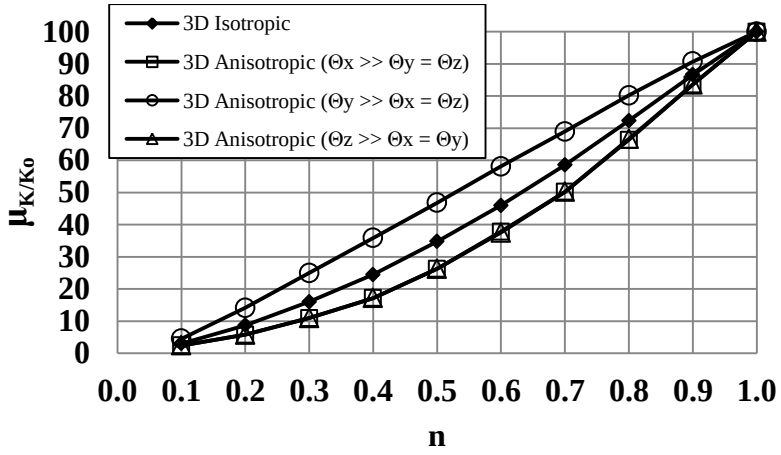

Figure 13 Comparison of the effective permeability obtained from 3D RFEM models (flow in the $y-$direction)

At the same porosity, the mean effective permeability of 3D anisotropic with high Θ_y is higher than results obtained from 3D isotropic and 3D anisotropic with high Θ_x and Θ_z. The results of 3D anisotropic with high Θ_x and Θ_z are the same but lower than 3D isotropic since the void shapes of 3D anisotropic with high Θ_x and Θ_z tend to be arranged perpendicularly to the flow direction.

9 COMPARING WITH 3D RFEM AND OTHER RESULTS

The theoretical results based on the effective medium theory and the experimental measurements of Doyen (1988) are compared in Figure 14, with the results from the current study using $\Theta = 0.1$. The theory is consistent with Kozeny-Carman formulas to calculate the permeability of Fontainebleau sandstone. The experiment test of sandstone was prepared from cores with porosity ranging from 5 to 22%. The definition of the effective permeability used in this study is defined in the classical geotechnical sense as the effective hydraulic conductivity with units of length/time. Therefore, in order to examine the influences of voids on an effective permeability analysis, the current results will be converted from the effective hydraulic conductivity to effective permeability, using a conversion formula based on the Carlile (Hively 1986) as follows

$$k = (K\frac{\mu}{\rho g})\bar{K} \tag{5}$$

where k is permeability (md), K is hydraulic conductivity (cm/s), μ is the dynamic viscosity of the fluid (0.0032 g/cm/s), ρ is the density of the fluid (1 g/cm^3), g is the acceleration due to gravity (980 cm/s^2) and the conversion unit from permeability (cm^2) to the millidarcy (md) $\approx 0.1013\text{x}10^{12}$. The hydraulic conductivity ($\bar{K}$) value of sandstone found in nature is given by 10^{-6} cm/s (Bear 1972).

In general, the permeability of sandstone ranges from 1 to 10000 md; therefore, any element assigned a random field value in the range $|Z| > z_{n/2}$ is treated as intact material a permeability with $K_0 = 1$, while any element where $|Z| \le z_{n/2}$ is treated as a void element with an assigned permeability of $K_0^{'} = 10,000$ (10000 times larger than the surrounding intact material) instead of $K_0^{'} = 100$. Following 1000 simulations, the normalized 3D RFEM results with the void element assigned $K_0^{'} = 10,000$ were computed for a range of variations of n = 0 to 0.3 and $\Theta = 0.1$. Thereafter, the results are converted to effective permeability (md) using Equation 5 for comparison with theoretical and experimental measurements as shown in Figure 14. From Figure 14, it can be observed that the current method gives similar values of the effective permeability to those given by the theoretical and experimental methods for all values of n.

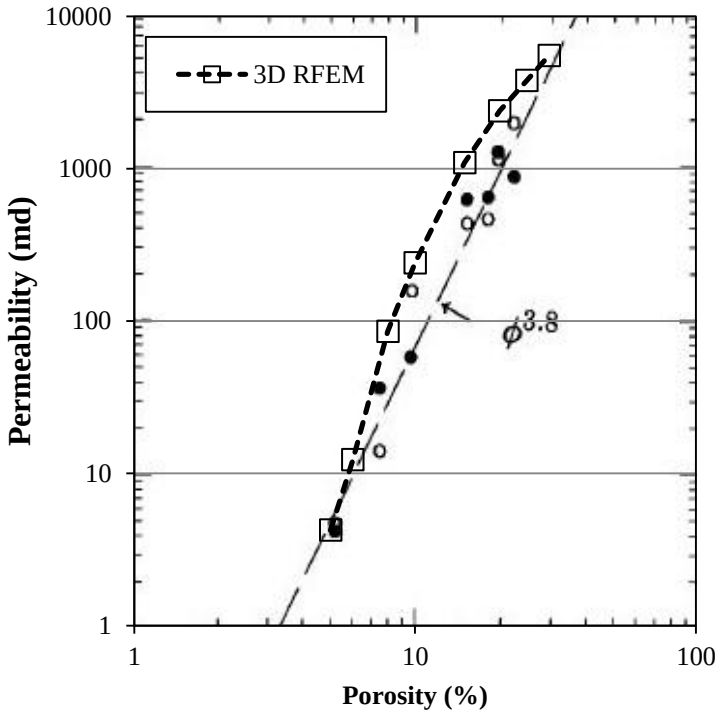

Figure 14 Comparison of the effective permeability obtained from 3D RFEM and the permeability of Fontainebleau Sandstone as a function of porosity. The solid circles represent the experimental measurements. The open circles represent the predicted values, based on the effective medium approximation (Doyen 1988). The open squares are from RFEM

The current results from Figure 14 are also compared with the site data of limestone and dolostone reservoirs from the Madison Formation (Ehrenberg el at., 2006). Follow Equation 5 based on the hydraulic conductivity ($\bar{K}$) value of limestone and dolostone found in nature = 10^{-8} cm/s (Bear 1972), it can be observed that the current method gives similar values of the effective permeability to those given by the site data for all values of n, as shown in Figure 15.

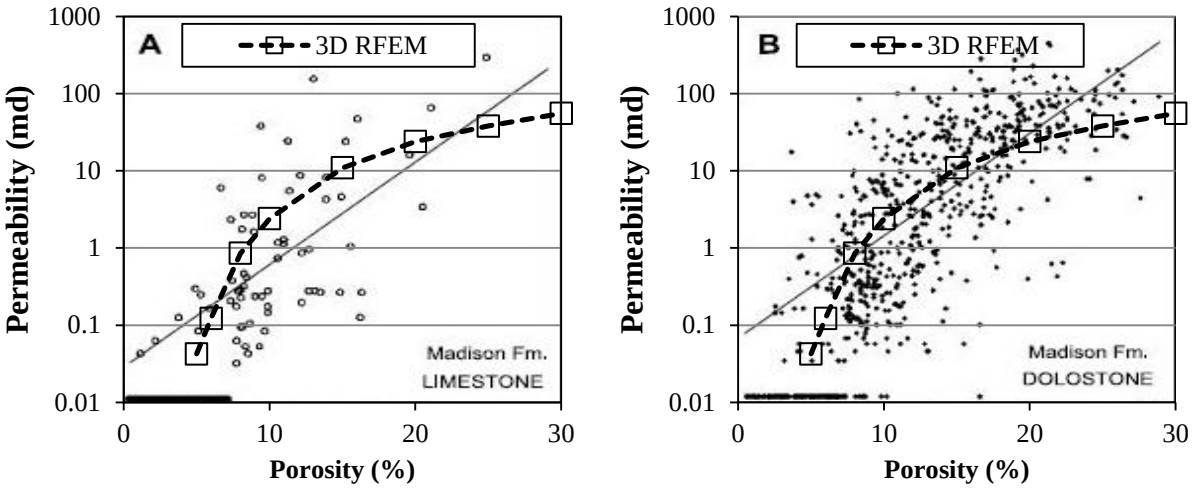

Figure 15 Comparison of the effective permeability obtained from 3D RFEM and the permeability from the Madison Formation as a function of porosity: (A) Limestones and (B) Dolostones. (Ehrenberg el at., 2006). The open squares are from RFEM

10 INFLUENCE OF VOID ELEMENT ON EFFECTIVE PERMEABILITY

There are only two different materials modeled in the finite element analysis. Each void is modeled explicitly as a material with significant higher permeability than the intact material $K_0 = 1$. As can be seen in Figure 16, for the case when $n = 0.2$, the results show a small influence due to the selected permeability of void elements. In the current work, a void permeability which is one hundred times larger than the intact material gives reasonable (and stable) results. It can be noted that a limiting value of permeability of void elements for numerical stability is equal to about 1×10^{19} for the software presented in this research.

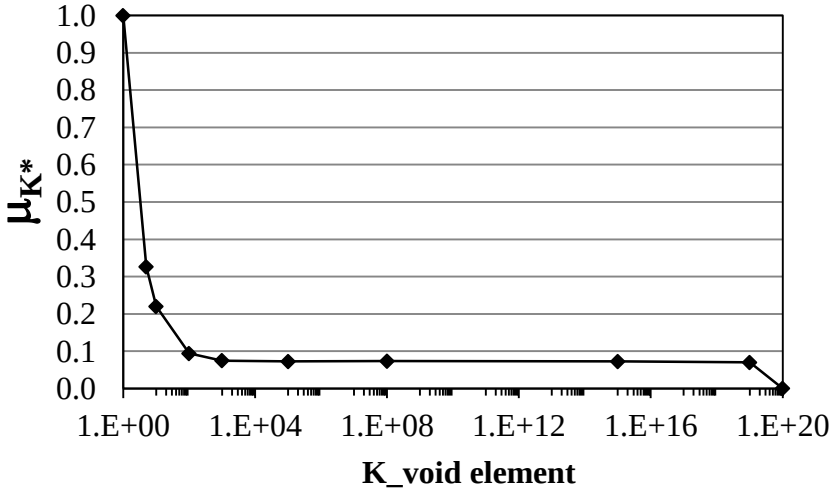

Figure 16 Influence of void element permeability on the normalized mean effective permeability. ($K^* = K / K_{\text{void element}}$)

Following each set of 1000 Monte-Carlo simulations, the mean of the normalized effective permeability were computed for a range of parametric variations of n and $K_{\text{void element}}$, with results shown in Figures 17. It can be noted that the mean normalized effective permeability increases towards one with increasing porosity n and that $K_{\text{void element}}$ has little influence.

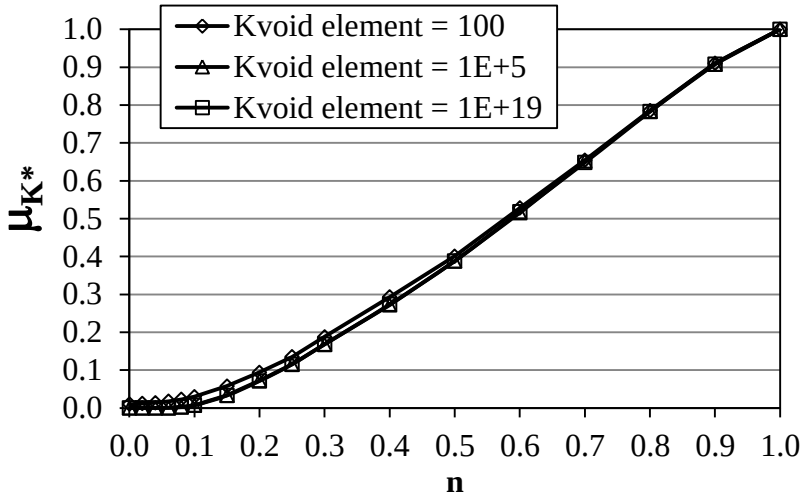

Figure 17 μ_{K^*} vs. n for $100 \le K_{\text{void element}} \le 1E+19$

11 CONCLUDING REMARKS

The random finite element method (RFEM) shows promise as a powerful alternative approach for modeling the mechanical influence of inclusions and voids in geomaterials. The RFEM together with Monte-Carlo simulations has been used in this study to investigate the influence of porosity and void size on the effective permeability of geomaterials containing random voids. The voids were not restricted to being simple shapes as in some of the theoretical methods, and the user could control the volume and size of inclusions through changes to the spatial correlation length. It was observed that while porosity had a significant effect on the effective permeability, the void size was less important. Anisotropic void structure was also investigated. It found that the effective permeability depended more on the direction of elongated voids than porosity. When the flow moved from the front left to the back right of the block test, the mean effective permeability had higher than the other directions of elongated voids. The study also investigated the RVE needed to capture the essential properties of a heterogeneous material containing voids. It was found that for the same porosity, the larger the size of the voids, the greater the size of the RVE. Finally, the paper presented favorable comparisons of the effective permeability in 3D with theoretical result and experimental measurements obtained by other investigators.

REFERENCES

[1]. Abedini, A, Torabi, F. and Tontiwachwuthikul, P., Reservoir rock type analysis using statistical pore size distribution. *Special Topics & Reviews in Porous Media. An International Journal*, 3(2), 97–103, 2011.

[2]. Barski, M. and Muc, A., Homogenization methods for two-phase composites. *Mechanics of Composite Materials*, Vol. 47, No. 4, 2011

[3]. Bear, J., Dynamics of fluids in porous media, *Dover Publications*, ISBN 0-486-65675-6, New York USA., 1972.

[4]. Bougeat, A., Homogenized behavior of two-phase flows in naturally fractured reservoirs with uniform fractures distribution. *Compute Method APPL MECH ENG*, vol. 47, no. 1-2, pp. 205-216, 1984.

[5]. Bosl, W.J., Dvorkin, J., Nur, A., A study of porosity and permeability using a lattice Boltzmann simulation. *Geophys. Res. Lett*. 25, 1475–1478, 1998.

[6]. Doyen, P.M., Permeability, Conductivity, and Pore Geometry of sandstone. *J. Geophysical research*, vol. 93, no. B7, p. 7729-7740, 1988.

[7]. Edie, Margaret S., Olsen, John F., Burns, Daniel R., and Toksoz, M. Nafi., Fluid flow in porous media: NMR imaging and numerical simulation. *MIT, Earth Resources Laboratory Industry Consortia Annual Report*, 2000-11

[8]. Ehrenberg, S.N., Eberli, G.P., Keramati, M. and Moallemi, S.A., Porosity-permeability relationships in interlayered limestone-dolostone reservoirs. *AAPG Bulletin*, v. 90, no. 1 (January 2006), pp. 91–114, 2005.

[9]. Fenton G.A. and Vanmarcke E.H., Simulation of random fields via local average subdivision, *J Eng Mech*, vol.116, no.8, pp. 1733-1749, 1990.

[10]. Fenton G.A. and Griffiths D.V., Statistics of block conductivity through a simple bounded stochastic medium, *Water Resour Res*, vol.29, no.6, pp.1825-1830, 1993.

[11]. Fenton G.A. and Griffiths D.V., Risk Assessment in Geotechnical Engineering, *John Wiley & Sons*, Hoboken, NJ, 2008.

[12]. Griffiths, D.V. and Fenton, G.A., Seepage beneath water retaining structures founded on spatially random soil, *Géotechnique*, 43(6), 577-587, 1993.

[13]. Griffiths, D.V. and Fenton, G.A., The random finite element method (RFEM) in steady seepage analysis., Chapter 10 in Probabilistic Methods in Geotechnical Engineering, eds. D.V. Griffiths and G.A. Fenton, *Pub. Springer Wien*, New York, pp.225–241, 2007.

[14]. Grucelski, A., Pozorski, J., Lattice Boltzmann simulation of fluid flowin porous media of temperature-affected geometry. *J. Theor. App. Mech*. 50, 193–214, 2012.

[15]. Guo, Z., Zhao, T.S., Lattice Boltzmann model for incompressible flows through porous media. *Phys. Rev*. E 66, 036304, 2002.

[16]. Hashin, Z., and S. Shtrikman, A variational approach to the theory of the elastic behavior of multiphase materials: *Journal of the Mechanics and Physics of Solids*, 11, 127–140, 1963.

[17]. Held, R., Attinger, S. and Kinzelbach, W., Homogenization and effective parameters for the Henry problem in heterogeneous formations. *Water resources research*, Vol. 41, W11420, 2005.

[18]. Hidajat, I., Singh, M., Cooper, J. and Mohanty, K., Permeability of Porous Media from Simulated NMR Response. *Kluwer Academic Publishers. Printed in the Netherlands. Transport in Porous Media* 48: 225–247, 2002.

[19]. Hively, Roger E., Independent Geologist. "Geological Aspects of the Codell Sandstone, Weld and Larimer Counties, Colorado, Document ID 13885-PA." *SPE Formation Evaluation (Society of Petroleum Engineers)* 1, no. 6 : 623-627, 1986.

[20]. Hoden, L. and O. Lia, A tensor estimator for the homogenization of absolute permeability: *Transport in porous media*, v.8, P.37-46, 1992.

[21]. Jin, G., Torres-Verdin, C., Toumelin, E., Comparison of NMR simulations of porous media derived from analytical and voxelized representations. *Journal of Magnetic Resonance*, 200 313–320, 2009.

[22]. Jiru, Z, Gaoling, T, Li, H. and Lun, Y., Porosity models for determining the pore-size distribution of rocks and soils and their applications. *Science China Press and Springer-Verlag Berlin Heidelberg* 2010 Vol.55 No.34: 3960–3970, 2010.

[23]. Kalam, M.Z., Digital Rock Physics for Fast and Accurate Special Core Analysis in Carbonates. *INTECH, New Technologies in the Oil and Gas Industry*, Chapter 9, p. 201-226, 2012.

[24]. Kate, J. M. and Gokhale, C. S., A simple method to estimate complete pore size distribution of rocks, *Eng. Geol*., vol.84**,** pp. 48–69, 2006.

[25]. Kimmich, R., Strange kinetics, porous media, and NMR. *Elsevier Science B.V. Chemical Physics* 284, p. 253–285, 2001.

[26]. Klusemann, B. and Svendsen, B., Homogenization methods for multi-phase elastic composites Comparisons and Benchmarks, *Technische Mechanik*, 30, 4, (2010), 374-386, 2009.

[27]. Liaw, H.K., Kulkarni, R., Chen, S. and Watson, A.T., Characterization of fluid distributions in porous media by NMR techniques. Materials, Inferfaces and Electrochemical Phenomena. *AIChE Journal*, Vol. 42, No. 2, 1996.

[28]. Liu, C., On the minimum size of representative volume element: An experimental investigation, *Exp Mech*, 45(3), pp.238-243, 2005.

[29]. Mercier, S., Molinari, A., Berbenni, S. and Berveiller, M., Comparison of different homogenization approaches for elastic-viscoplastic materials. *Modelling Simul. Mater. Sci. Eng*. 20, 024004 (22p), 2012.

[30]. Muc, A. and Barski, M., Homogenization, Numerical Analysis & Optimal Design of MR Fluids. *Advanced Materials Research*, Vols. 47-50 pp 1254-1257, 2008.

[31]. Ostoja-Starzewski, M., X. Du, Khisaeva, Z.F. and Li, W., On the size of Representative Volume Element in Elastic, Plastic, Thermoelastic and Permeable Random Microstructures. *Materials Science Forum*, Vols. 539-543 pp 201-206, 2007.

[32]. Paiboon J. Griffiths D.V. Huang J. and Fenton G.A., Numerical analysis of effective properties of geomaterials containing voids using 3D random fields and finite elements. *International Journal of Solids and Structures*, vol.50, no.20-21, pp.3233-3241, 2013.

[33]. Popov, P., Efendiev, Y., and Qin, G., Multiscale Modeling and Simulations of Flows in Naturally Fractured Karst Reservoirs. *Commun. Comput. Phys. In press*, 2008.

[34]. Pouya, A. and Vu, M., Fluid flow and effective permeability of an infinite matrix containing disc-shaped cracks. *Advances in Water Resources*, 42 37–46, 2012.

[35]. Pozdniakov, S., Tsang, C.-F., A self-consistent approach for calculating the effective hydraulic conductivity of a binary, heterogeneous medium. *Water Resour. Res*. 40, W05105, 2004.

[36]. Hinton, E., Sienz, J., & Afonso, S. M. B., Experiences with Olhoff's 'exact' semi-analytical algorithm. In Olhoff, N. & Rozvany, G. I. N., eds, *First World Congress of Structural and Multidisciplinary Optimization (WCSMO-1*), pp. 41–46, 1995.

[37]. Ramm, E., Strategies for tracing the nonlinear response near limit points. In Wunderlich, W., Stein, E., & Bathe, K. J., eds, *Nonlinear Finite Element Analysis in Structural Mechanic*s, pp. 63–89. Springer-Verlag, 1981.

[38]. Ramstad, T., Idowu, N. and Nardi, C., Relative permeability calculations from two-phase flow simulations directly on digital images of porous rocks. *Transp Porous Med* 94:487–504, 2012.

[39]. Saez, A. E., C. J. Otero, and I. Rusinek, The effective homogeneous behavior of heterogeneous porous media: *Transport in Porous Media*, v. 4, p. 213–238, 1989.

[40]. Sharp, B., DesAutels, D., Power, G., Young, R. Noble Energy Inc., Foster, S., Diaz, E. and Dvorkin, J., *World oil, reservoir characterization*. P. 67-68, 2009.

[41]. Sørland, G.H., Djurhuus, K., Widerøe, H.C., Lien, J.R. and Skauge, A., Absolute pore size distributions from NMR. *The Open-Access Journal for the Basic Principles of Diffusion Theory, Experiment and Application. Diffusion Fundamentals* 5 4.1 - 4.15, 2007.

[42]. Smith, I.M., Griffiths, D.V., and Margetts, L., Programming the finite element method, *John Wiley and sons, Chichester*, New York, 5th edition, 2014.

[43]. Szymkiewicz, A., Calculating Effective Conductivity of Heterogeneous Soils by Homogenization. *Archives of Hydro-Engineering and Environmental Mechanics*, Vol. 52 (2005), No. 2, pp. 111–130, 2005.

[44]. Waki, H., et al., Estimation of effective permeability of magnetic composite materials. *IEEE TRANSACTIONS ON MAGNETICS*, VOL. 41, NO. 5, 2005.

[45]. White, Joshua A., Borja, Ronaldo I., and Fredrich, Joanne T., Calculating the effective permeability of sandstone with multiscale lattice Boltzmann/finite element simulations. *Acta Geotechnica*, 1:195–209, 2006.

[46]. Zhang, T., Hurley, N.F., Zhao, W. and Schlumberger-Doll research., Numerical modeling of heterogeneous carbonates and multi-scale dynamics. *SPWLA 50th Annual Logging Symposium*, June 21-24, 2009.

[47]. Zhang, X., Lattice Boltzmann implementation for fluids flow simulation in porous media. *IJIGSP* 3, 39–45, 2011.

Acknowledgements

The authors wish to acknowledge the support of (i) NSF grant CMMI-0970122 on "GOALI: Probabilistic Geomechanical Analysis in the Exploitation of Unconventional Resources", and (ii) The Royal Thai Government.